

## Irradiance and the elemental stoichiometry of marine phytoplankton

Z. V. Finkel<sup>1</sup> and A. Quigg<sup>2</sup>

Institute of Marine and Coastal Sciences, Rutgers University, New Brunswick, New Jersey 08901

J. A. Raven

Plant Research Unit, University of Dundee at SCRI, Scottish Crop Research Institute, Invergowrie, Dundee, United Kingdom DD2 5DA

J. R. Reinfelder

Department of Environmental Science, Rutgers University, New Brunswick, New Jersey 08901

O. E. Schofield

Institute of Marine and Coastal Sciences, Rutgers University, New Brunswick, New Jersey 08901

P. G. Falkowski

Institute of Marine and Coastal Sciences and Department of Geology, Rutgers University, New Brunswick, New Jersey 08901

### Abstract

We analyzed the elemental composition (C, N, P, S, K, Mg, Ca, Sr, Fe, Mn, Zn, Cu, Co, Mo, and Ni) of five marine phytoplankton species representing the four major marine phyla grown over a range of growth irradiances. We found substantial variability in the elemental composition between different species, which is consistent with previously reported differences associated with evolutionary history. We found that many elements (Fe, Mn, Zn, Cu, and Mo) are enriched relative to phosphorus by about two to three orders of magnitude under irradiances that are limiting for growth, and net steady-state uptake of element:P is often elevated under lower irradiances. For most elements, the variability in element:P due to irradiance is comparable to the variability due to phylogenetic differences at any irradiance, but often the interaction between genetic differences and the phenotypic response to irradiance amplifies the differences in elemental composition between species. The fractionation of trace elements relative to phosphorus into phytoplankton biomass under low light is consistent with depleted levels of Cu<sup>2+</sup> and Mn<sup>2+</sup> in deep chlorophyll maxima, suggesting that the export of low-light-acclimated phytoplankton is a major source of trace element flux to the deep ocean and an important factor in the biogeochemical cycles of many of the biologically limiting elements in the oceans.

In the first half of the 20th century Alfred Redfield and Richard Fleming established that marine plankton have a relatively constrained elemental ratio of 106C:16N:1P atoms (Redfield 1934, 1958; Fleming 1940) that is remarkably similar to the ratio of dissolved fixed inorganic nitrogen to phosphate in seawater. These observations led to the paradigm that on average, phytoplankton will

consume inorganic nitrogen and phosphate in proportion to their availability in surface waters, converting them into cellular biomass that is eventually returned into their inorganic forms through decomposition. The Redfield ratio concept has been used extensively in biogeochemical models to link phytoplankton production and the carbon cycle to the nitrogen and phosphorus cycles. Associated with the increasing recognition that trace elements such as iron can limit primary production (Martin 1992) there has been an effort to extend the Redfield ratio to Si and the micronutrients (Brzezinski 1985; Bruland et al. 1991; Ho et al. 2003) and to understand the physiological, ecological, biogeochemical, and evolutionary factors that contribute to the elemental stoichiometry of marine organisms and seawater (Falkowski 2000; Quigg et al. 2003; Klausmeier et al. 2004).

A recent analysis of major nutrients and trace elements in 29 algal species from the major phylogenetic groups under uniform culture conditions indicated that there are systematic phylogenetic differences in the elemental composition of phytoplankton (Quigg et al. 2003; Falkowski et al. 2004). On the basis of an analysis of available

<sup>1</sup>Current address: Environmental Science Program, Mount Allison University, Sackville, New Brunswick, Canada E4L 1A7.

<sup>2</sup>Current address: Department of Marine Biology, Texas A&M University, Galveston, Texas 77551.

### Acknowledgments

We thank F. F. M. Morel, T-Y. Ho, and CEBIC for their role in the early phase of this project, R. Sherrell and Paul Field with their assistance with ICPMS, C. Fuller and K. Wyman for their help with CHN, R. Chiampi for her help with sampling, and R. Armstrong, B. Sunda, A. J. Irwin, and three anonymous reviewers for useful comments.

This work was supported by an NSF biocomplexity grant (ERUPT, OCE-0084032) to P.G.F. and O.E.S. and an EPA STAR Fellowship (F4E20409), NSERC, and NBIF funding to Z.V.F.

experimental data, Ho et al. (2003) deduced that phenotypic differences in elemental composition due to environmental conditions such as irradiance, macronutrient concentration, and micronutrient concentration rarely result in more than two- to fivefold variability in element (E):P in response to an order-of-magnitude variation in irradiance or macronutrient concentration, or an order-of-magnitude variability for over three orders-of-magnitude variation in trace metal concentrations. On this basis Quigg et al. (2003) and Ho et al. (2003) hypothesize that phenotypic variation in elemental stoichiometry is much smaller than genetic differences between phylogenetic groups, leading to the hypothesis that differences in elemental composition among species primarily represent phylogenetic differences in biochemical requirements and the ability of the organisms to take up and store these elements, not environmental or culture conditions.

Elemental stoichiometry can be strongly affected by the magnitude of photosynthetically active radiation and photoperiod. Current theory predicts that a change in growth irradiance will affect the cellular concentration of elements that are required for light harvesting and oxygenic photosynthesis: N, Fe, and to a lesser extent Mn (Raven 1990; Sunda and Huntsman 1997, 2004) and elements associated with a change in growth rate such as N and P (Sterner and Elser 2002). Experimental studies on diatoms, prymnesiophytes, and dinoflagellates indicate that a decrease in growth irradiance can result in an increase in the cellular concentration of Fe and Mn, which have a critical role in light harvesting and photosynthesis (Sunda and Huntsman 1997, 1998a). Surprisingly few studies have been conducted to look at the change in elements other than C, N, P, or Fe as a function of growth irradiance. Recently Sunda and Huntsman (2004) found that the cellular concentration of Zn increased with decreasing light period in the coastal diatom *Thalassiosira pseudonana*. This suggests that elements not intimately associated with light harvesting may also be affected by growth irradiance. No work has simultaneously examined the effect of irradiance on a large range of major biologically required elements in phytoplankton.

We analyzed the elemental composition, C, N, P, S, K, Mg, Ca, Sr, Fe, Mn, Zn, Cu, Co, Mo, and Ni, of five marine phytoplankton species representing four major marine phyla over a light gradient to test two hypotheses: (1) growth irradiance is responsible for a relatively small proportion of the total variability in the elemental stoichiometry of phytoplankton, and that (2) growth irradiance will preferentially alter the cellular concentrations of elements specifically associated with light harvesting and growth rate.

## Materials and methods

**Culturing and sampling**—Phytoplankton species investigated in this study included one nitrogen-fixing cyanobacterium *Cyanothece* sp. (WH8904, provided by Dr. J. Waterbury), a prasinophyte, *Pycnococcus provasolii* (CCMP 1203), a dinoflagellate, *Amphidinium carterae* (CCMP 1314), and two members of the Bacillariophyceae:

*Thalassiosira weissflogii* (CCMP 1336) and *Chaetoceros calcitrans* (CCMP 1315). The algae were grown at  $19^{\circ}\text{C} \pm 1^{\circ}\text{C}$  using a 12:12 light:dark cycle at five irradiances: quanta of 15, 30, 100, 250, and  $500 \mu\text{mol m}^{-2} \text{s}^{-1}$ . All species were cultured in the synthetic seawater medium Aquil, which has a fixed nitrogen source, as described in Ho et al. (2003). Each experimental species was maintained in exponential growth through a minimum of six generations before harvesting (Fogg and Thake 1987). For most irradiance treatments three replicate bottles were maintained for each species; in a few cases, due to experimental difficulties such as trace metal contamination or experimental error, there were only one or two replicate bottles for certain treatments, and in the case of  $250 \mu\text{mol m}^{-2} \text{s}^{-1}$  treatment, some species had more than three replicate bottles, and no growth rate measurements were available for *Cyanothece* sp. (Table 1). Cell size and the number of cells per unit volume of media were determined with a calibrated Beckman Multisizer Coulter Counter (II) and these measurements were used to calculate growth rates.

**Elemental analysis**—All elements but carbon and nitrogen were assayed with sector field high-resolution inductively coupled plasma mass spectrometry (HR-ICPMS, Element, ThermoFinnigan) fitted with a self-aspirating microflow Teflon nebulizer (PFA-100, Elemental Scientific Inc.) and a quartz Scott-type double pass spray chamber. Methodological details are provided in Ho et al. (2003) and Quigg et al. (2003). Carbon and nitrogen analysis were obtained by filtering 25–50-mL culture samples onto precombusted 13-mm Gelman AE GF filters. These were analyzed for C and N content using a Carlo Erba elemental analyzer.

All E:P ratios were averaged, then log-transformed to homogenize the variance. Observations from  $250 \mu\text{mol m}^{-2} \text{s}^{-1}$  quanta treatment have been previously published in Ho et al. (2003) and Quigg et al. (2003) and are reported here for comparison to the other light treatments. Outliers were identified and removed if: one of the replicates differed by more than one order of magnitude from the other ( $>2$ ) replicates, and as a result  $\log(\text{E}:\text{P})$  at  $250 \mu\text{mol m}^{-2} \text{s}^{-1}$  for *P. provasolii*, *A. carterae*, and *T. weissflogii* differ slightly from those reported in Ho et al. (2003); if the filter or acid blank showed evidence of contamination; or if the element was below the detection limit of our method. Often Ni was below the detection limit of our method, and we were unable to get triplicate measurements for all irradiances and for all species, but because Ni measurements are so sparse in the literature we decided to include the 36 successful measurements obtained but did not include Ni in any of the statistical analyses used to determine the proportion of the variance in E:P due to phylogenetic effects and phenotypic response to irradiance.

**Data analyses**—To quantify and partition the magnitude and variability in  $\log(\text{E}:\text{P})$  due to phylogeny and phenotype we use three main types of data analyses: (1) principal component analysis; (2) an examination of the maximum divided by the minimum E:P; (3) an analysis of variance (ANOVA). First, principal component analysis

Table 1. Geometric mean E : P of marine phytoplankton as a function of growth irradiance (I, quanta,  $\mu\text{mol m}^{-2} \text{s}^{-1}$ ). The unit for C, N, S, K, Mg, and Ca is mol (mol P)<sup>-1</sup>, and for Sr, Fe, Mn, Zn, Cu, Mo, and Ni is mmol (mol P)<sup>-1</sup> with 1 SE (%) in brackets. The 250  $\mu\text{mol m}^{-2} \text{s}^{-1}$  quanta treatment is from Quigg et al. (2003). If there was only one replicate no standard error is reported; \* indicates two replicates, and † refers to more than three replicates, respectively. Growth rate (1 SE) is reported as day<sup>-1</sup>, and P is cell quota in femtomoles of P.

| Taxa                             | I   | $\mu$       | P quota        | C : P          | N : P         | S : P         | K : P         | Mg : P        | Ca : P        | Sr : P         | Fe : P         | Mn : P         | Zn : P          | Cu : P         | Co : P        | Mo : P         | Ni : P         |
|----------------------------------|-----|-------------|----------------|----------------|---------------|---------------|---------------|---------------|---------------|----------------|----------------|----------------|-----------------|----------------|---------------|----------------|----------------|
| <i>Thalassiosira weissflogii</i> | 15  | 0.13 (1.8)  | 96.725 (7.8)   | 201.574 (9.3)  | 41.027 (8.2)  | 0.768 (23.2)  | 2.627 (11.3)  | 1.548 (2.2)   | 0.138 (10.1)  | 1.278 (9.7)    | 14.727 (5.9)   | 4.291 (3.5)    | 1.617 (24.4)    | 0.485 (7.8)    | 0.142 (9.3)   | 0.058 (11.0)   |                |
|                                  | 30  | 0.16 (0.2)  | 184.254 (22.5) | 70.054 (37.2)  | 13.787 (42.6) | 0.863 (12.3)  | 2.264 (13.9)  | 1.076 (4.7)*  | 0.119 (1.1)*  | 1.038 (15.0)   | 12.287 (1.3)   | 4.376 (4.0)    | 1.988 (32.6)    | 0.527 (13.6)   | 0.148 (14.7)* | 0.024 (19.7)   |                |
|                                  | 100 | 0.39 (11.7) | 102.162 (8.9)  | 79.577 (5.6)   | 14.857 (3.7)  | 1.032 (10.1)  | 1.337 (6.7)*  | 0.389 (1.3)   | 0.192 (13.4)* | 1.001 (19.3)   | 5.214 (7.8)*   | 5.092 (17.2)   | 3.345 (33.4)    | 0.380 (8.7)    | 0.049 (47.5)  | 0.047 (21.9)   | 1.741          |
|                                  | 250 | 0.96        | 130.265 (7.2)  | 83.232 (7.0)†  | 13.113 (7.1)† | 1.317 (17.4)  | 0.529 (5.9)   | 0.244         | 0.369 (38.5)  | 2.710 (13.7)   | 1.581 (14.4)†  | 5.304 (1.4)†   | 0.711 (3.3)†    | 0.171 (2.6)†   | 0.100 (0.9)†  | 0.013 (14.5)†  | 0.021 (91.2)*  |
|                                  | 500 | 0.30 (0.4)  | 275.263 (10.3) | 41.642 (40.2)  | 7.793 (40.6)  | 0.797 (4.0)   | 0.724 (9.5)   | 0.143 (7.4)   | 0.055 (7.3)   | 0.817 (10.8)   | 15.462 (1.8)   | 4.557 (2.6)    | 0.789 (25.5)    | 0.092 (5.7)*   | 0.072 (1.9)   | 0.017 (8.0)    |                |
| <i>Pyrococcus</i>                | 15  | 0.26 (4.0)  | 1.774 (74.2)   | 69.977 (80.2)  | 10.954 (74.2) | 0.590 (8.3)*  | 0.681 (45.5)  | 1.228 (7.4)*  | 0.309 (12.6)* | 20.389 (17.2)* | 52.104 (87.0)  | 4.043 (29.1)   | 25.904 (50.5)   | 2.399 (31.6)*  | 0.116         | 0.118 (24.5)*  | 3.894          |
| <i>provasoli</i>                 | 30  | 0.36 (0.6)  | 1.111 (20.6)   | 108.833 (18.9) | 15.793 (20.7) | 1.402 (10.5)* | 1.303 (3.9)*  | 3.578 (57.2)* | 0.517         | 2.459 (125)    | 43.722 (8.4)   | 2.407 (2.1)    | 8.374 (17.6)    | 2.369 (80.9)*  | 0.030 (10.3)  | 0.023 (72.5)   | 0.684 (32.2)   |
|                                  | 100 | 0.56 (0.6)  | 1.572 (8.1)    | 112.136 (14.5) | 12.294 (15.4) | 1.884 (9.5)*  | 0.419 (0.9)*  | 1.399 (20.4)* | 0.156 (34.7)* | 0.616 (63.7)*  | 44.695 (0.9)   | 2.402 (2.0)    | 7.035 (15.7)    | 0.112 (82.7)*  | 0.027 (20.9)* | 0.035 (40.4)   | 1.597 (23.7)*  |
|                                  | 250 | 0.63        | 0.734 (1.6)    | 192.037 (2.9)† | 27.162 (3.2)† | 1.300 (1.2)†  | 1.415 (9.4)†  | 0.128 (2.5)†  | 0.208 (11.8)† |                | 12.014 (7.5)†  | 2.050 (2.1)†   | 0.860 (8.3)†    | 0.512 (8.5)†   | 0.088 (2.9)†  | 0.005 (21.4)†  | 0.057 (11.1)†  |
|                                  | 500 | 0.80 (16.3) | 1.952 (15.2)   | 116.881 (19.4) | 14.962 (21.4) | 0.793 (1.3)   | 0.152 (3.2)   | 0.406 (14.5)  | 0.242 (12.3)  | 0.777 (16.0)   | 8.673 (0.7)*   | 1.331 (31.3)*  | 0.400 (30.7)*   | 0.173 (28.2)*  |               | 0.007 (117.7)* |                |
| <i>Cyanoditice</i>               | 15  | 0.25 (10.9) | 1.083 (7.0)    | 135.008 (16.6) | 21.957 (19.1) | 0.886 (6.4)   | 1.396 (12.2)  | 0.753 (15.2)  | 0.368 (18.9)  | 3.844 (8.0)*   | 1053.42 (8.6)  | 57.179 (7.6)   | 72.040 (12.5)   | 1058.937 (8.0) | 0.148 (14.2)  | 0.169 (0.5)*   | 243.797 (16.2) |
| sp.                              | 30  | 0.39 (6.1)  | 1.898 (30.0)   | 80.2130 (38.9) | 10.906 (31.7) | 3.122 (5.2)   | 1.489 (12.2)  | 2.610 (11.2)  | 0.406 (11.3)  | 2.985 (11.6)*  | 48.209 (13.3)  | 18.332 (13.8)  | 9.264 (1.4)     | 1.718 (21.0)*  | 0.455 (11.1)* | 0.037 (16.9)*  | 3.396 (6.8)*   |
|                                  | 100 | 0.48 (2.0)  | 1.459 (6.3)    | 67.818 (6.6)   | 14.999 (3.2)  | 1.145 (4.7)   | 1.145 (6.2)   | 1.770 (49.4)* | 0.893 (0.6)*  | 2.248 (14.4)   | 11.189 (25.6)  | 1.750 (29.1)   | 5.094 (32.5)    | 0.668 (7.1)    | 0.098         |                |                |
|                                  | 250 |             | 0.259 (5.5)    | 44.510 (10.5)† | 13.320 (5.5)† |               |               |               |               | 7.117 (9.6)†   |                | 0.301 (6.5)†   | 1.057 (13.8)†   | 0.230 (6.4)†   | 0.010 (2.9)†  | 0.035 (4.1)†   | 0.115 (5.1)†   |
|                                  | 500 | 0.74 (0.9)  | 15.272 (10.8)  | 14.032 (10.8)  | 1.462 (10.8)  | 1.017 (2.5)   | 0.601 (1.9)   | 0.551 (5.7)   | 0.929 (2.7)   | 0.858 (3.4)    | 7.676 (5.3)    | 0.794 (19.9)*  | 1.140 (15.0)    | 0.277 (0.8)    | 0.032         | 0.014 (5.7)    | 0.051 (41.2)*  |
| <i>Amphidinium carterae</i>      | 15  | 0.14 (1.2)  | 48.115 (3.6)   | 196.060 (8.7)  | 26.018 (9.7)  |               |               | 0.395 (29.0)  | 0.519 (6.1)*  | 1.334 (24.6)   | 359.265 (27.5) | 175.621 (11.3) | 137.998 (18.1)* | 331.921 (12.3) | 2.614 (4.7)*  | 0.139 (22.0)   | 5.267 (22.3)*  |
|                                  | 30  | 0.27 (2.2)  | 66.791 (5.5)   | 114.246 (22.5) | 14.331 (28.4) | 1.689 (21.2)  | 0.595 (16.4)  | 1.022 (14.3)* | 0.161 (26.5)  | 1.142 (15.9)   | 20.547 (29.4)  | 4.490 (37.3)   | 4.120 (31.2)    | 0.569 (8.7)*   | 0.201 (83.9)* | 0.014 (61.4)*  |                |
|                                  | 100 | 0.46 (3.6)  | 65.212 (34.8)  | 105.135 (37.4) | 14.092 (37.2) | 1.328 (4.4)*  | 0.602 (11.3)* | 0.268         | 0.477 (29.2)* | 2.179 (25.0)   | 29.923 (6.7)*  | 3.560 (14.1)   | 6.625 (36.2)*   | 1.609 (16.9)*  | 0.182 (58.0)* | 0.019 (65.2)*  |                |
|                                  | 250 | 0.52        | 55.751 (5.3)   | 125.819 (5.8)† | 18.510 (6.1)  | 1.416 (6.4)†  | 0.103 (21.4)* | 0.327 (8.1)   | 0.255 (11.5)  | 1.128 (5.4)†   | 18.775 (33.3)  | 5.133 (4.0)    | 1.177 (33.4)    | 0.510 (15.2)   | 0.364 (3.3)   | 0.179 (2.6)    | 0.049 (86.0)*  |
|                                  | 500 | 0.59 (1.6)  | 34.228 (18.5)  | 161.299 (18.6) | 20.934 (18.2) | 1.558 (3.0)*  | 0.180 (18.5)* | 0.326 (27.8)  | 0.091 (9.8)   | 1.164 (18.5)   | 39.009 (3.0)   | 7.147 (0.9)    | 0.645 (40.8)*   | 0.203 (31.3)   | 0.258 (14.4)  | 0.036 (8.6)    |                |
| <i>Chaetoceros</i>               | 15  | 0.21 (7.3)  | 1.440 (46.7)   | 148.670 (46.7) | 21.589 (49.7) |               |               |               | 0.055 (32.1)* | 6.528 (2.6)*   | 520.705 (0.5)  | 238.979 (4.0)* | 39.900 (10.3)*  | 209.616 (6.5)  | 0.220 (35.9)  | 0.598 (60.4)   | 76.590 (22.8)  |
| <i>calchitans</i>                | 30  | 0.30 (0.8)  | 2.754 (4.12)   | 93.230 (9.8)   | 10.930 (7.7)  |               | 0.533 (5.7)   | 0.813 (3.9)   | 0.173 (9.1)   | 2.104 (4.1)    | 25.227 (9.4)   | 2.357 (7.1)    | 8.808 (2.7)*    | 0.243 (36.2)   | 0.015 (75.6)  | 0.017 (21.7)   | 0.324 (52.6)*  |
|                                  | 100 | 0.59 (1.3)  | 3.499 (44.4)   | 59.983 (37.9)  | 8.029 (37.9)  | 0.602 (46.8)* | 0.184         | 0.309 (42.3)  | 0.155         | 2.930 (46.5)*  | 14.005 (15.8)  | 1.263 (20.3)   | 5.822 (70.9)*   | 0.230 (15.7)*  | 0.018 (17.5)  | 0.040 (122.7)* | 0.308 (19.0)   |

Table 2. Correlations between cell size (cell volume  $V$  [ $\mu\text{m}^3$ ]) and cellular C, N, and P (mol), all are highly significant ( $n = 94$ ,  $p < 0.0001$ ).

| Elements |   | $R$  |
|----------|---|------|
| P        | C | 0.80 |
| P        | N | 0.79 |
| P        | V | 0.86 |
| V        | C | 0.89 |
| V        | N | 0.87 |
| N        | C | 0.98 |

(PCA) is used to determine the proportion of total variance in the data that can be described by a small number of linear combinations of predictor variables. Each principal component is a linear combination of  $\log(E_1:P)$ ,  $\log(E_2:P)$ , ...,  $\log(E_n:P)$ , ordered so that each component explains the maximum amount of residual variance. The representation of the data on the two principal component axes permits a visualization of the maximum amount of variability possible from a projection of the data onto a plane. The PCA biplot presents a vector along each  $\log(E:P)$  axis projected onto the plane. The composition of each principal component can be recovered by projecting each vector onto the respective axis. In addition, the taxonomic affiliation and light treatment are indicated through the use of color and shape of the data points on the plot. Second, the maximum variability in  $E:P$  was assessed by calculating the maximum  $\times$  minimum<sup>-1</sup> for each  $\log(E:P)$  over all species and irradiance treatments (total or maximum variability in  $\log[E:P]$ ). Third, a two-way ANOVA was used to quantify and evaluate the statistical significance of phylogeny, phenotypic response to irradiance, and the interaction of phylogeny and phenotype as factors predicting variation in each  $\log(E:P)$  and log net steady-state uptake (mol E [mol P h]<sup>-1</sup>), separately (Tables 3 and 4). Most species-treatment combinations had three replicates, but because of experimental and analytical difficulties, the design was not completely balanced (orthogonal). As a result, the sums of squares

for each of the main effects depended on the order in which they were included in the model (Sokal and Rohlf 1994). For our data this amounted to only a small (<5%) variation; analyses reported are an average of the two possible models. The PCA and ANOVA analyses were performed with R (R Development Core Team 2005).

## Results

The antilog of the mean of the log-transformed  $E:P$  (geometric mean) measured for the five different species of marine phytoplankton as a function of growth irradiance are presented in Table 1 and all replicates are reported in Web Appendix 1 ([http://www.aslo.org/lo/toc/vol\\_51/issue\\_6/2690a1.pdf](http://www.aslo.org/lo/toc/vol_51/issue_6/2690a1.pdf)). Elemental ratios are only available for three irradiances, 15, 30, and 100  $\mu\text{mol m}^{-2} \text{s}^{-1}$  quanta for *C. calcitrans* because this species did not grow at 250 and 500  $\mu\text{mol m}^{-2} \text{s}^{-1}$  under our growth conditions. In this study, cellular P, N, C, and cell volume are all highly correlated, indicating that most trends in  $E:P$  will also apply to E normalized to cell volume or carbon (Table 2). Normalization to P is preferred since it was measured simultaneously with the majority of the elements using ICPMS. Recent results on *Trichodesmium* spp. and two diatom cultures indicate that phosphorus can accumulate on the outside of phytoplankton cells (Sañudo-Wilhelmy et al. 2004), although in *T. pseudonana* grown in *fl2*, less than 40% of total P was associated with the cell wall, plasmalemma, and nuclei (Reinfelder and Fisher 1991). If phosphorus accumulated on the surface of the phytoplankton in this study, then  $E:P$  may be underestimated, but the correlation of cellular P with C, N, and cell volume indicate that all the trends among species and with irradiance are robust (Table 2).

*Genetic differences versus phenotypic response in log(E:P) over a range of growth irradiance*—A PCA using the correlations between  $\log(E:P)$  was used to visualize the relative effect of genetic differences and phenotypic response to growth irradiance on two groupings of elements:

Table 3. Two-way analysis of variance of  $\log(E:P)$  as a function of taxonomic differences (phylogenetic effect), irradiance (phenotypic effect), and the interaction (phenotypic  $\times$  phylogenetic effect) between these two effects (reported as a percentage of total sum of squares [SS]). Total SS is the total sum of squared deviation from the mean for the data,  $p < 0.001$  for all  $E:P$ , and  $n$  is the total number of observations.

|                     | Phylogenetic effect % | Phenotypic effect % | Interaction % | Residual error % | Total SS | Total $n$ |
|---------------------|-----------------------|---------------------|---------------|------------------|----------|-----------|
| $\log(C:P)$         | 34                    | 16                  | 31            | 20               | 7.28     | 95        |
| $\log(N:P)$         | 15                    | 26                  | 39            | 20               | 7.04     | 95        |
| $\log(S:P)$         | 26                    | 34                  | 30            | 11               | 1.78     | 59        |
| $\log(K:P)$         | 36                    | 30                  | 31            | 4                | 7.63     | 56        |
| $\log(\text{Mg}:P)$ | 14                    | 58                  | 23            | 4                | 9.76     | 58        |
| $\log(\text{Ca}:P)$ | 47                    | 7                   | 41            | 6                | 6.15     | 58        |
| $\log(\text{Sr}:P)$ | 17                    | 29                  | 45            | 9                | 6.38     | 60        |
| $\log(\text{Fe}:P)$ | 20                    | 55                  | 23            | 3                | 30.69    | 74        |
| $\log(\text{Mn}:P)$ | 15                    | 43                  | 40            | 1                | 32.36    | 75        |
| $\log(\text{Zn}:P)$ | 13                    | 67                  | 16            | 4                | 30.41    | 72        |
| $\log(\text{Cu}:P)$ | 11                    | 63                  | 26            | 1                | 81.71    | 70        |
| $\log(\text{Co}:P)$ | 40                    | 23                  | 32            | 4                | 20.37    | 64        |
| $\log(\text{Mo}:P)$ | 19                    | 43                  | 29            | 9                | 17.87    | 68        |

Table 4. Two-way analysis of variance of log steady-state uptake rate ( $\text{mol E} [\text{mol P h}]^{-1}$ ) as a function of irradiance (phenotypic response) and taxonomic differences (phylogenetic effect), and the interaction between these two effects (%). Total SS is the total sum of squared deviation from the mean for the data,  $p \ll 0.001$  for all E:P, and  $n$  is the total number of observations.

|    | Phylogenetic effect % | Phenotypic effect % | Interaction % | Residual error % | Total SS | Total $n$ |
|----|-----------------------|---------------------|---------------|------------------|----------|-----------|
| C  | 19                    | 40                  | 25            | 16               | 9.28     | 88        |
| N  | 14                    | 41                  | 28            | 17               | 9.10     | 88        |
| S  | 18                    | 55                  | 23            | 5                | 5.69     | 59        |
| K  | 47                    | 15                  | 32            | 6                | 5.50     | 56        |
| Mg | 29                    | 32                  | 33            | 6                | 8.11     | 58        |
| Ca | 38                    | 29                  | 29            | 4                | 11.21    | 58        |
| Sr | 26                    | 14                  | 52            | 8                | 8.25     | 60        |
| Fe | 37                    | 26                  | 33            | 4                | 20.22    | 66        |
| Mn | 14                    | 28                  | 56            | 2                | 17.15    | 68        |
| Zn | 29                    | 36                  | 30            | 5                | 20.11    | 65        |
| Cu | 21                    | 49                  | 30            | 1                | 62.25    | 63        |
| Co | 44                    | 26                  | 23            | 7                | 12.81    | 57        |
| Mo | 18                    | 26                  | 44            | 12               | 12.75    | 61        |

the trace metals Fe:P, Mn:P, Zn:P, Cu:P, Co:P, Mo:P; and the macronutrients and alkali and alkaline earth metals: C:P, N:P, S:P, K:P, Mg:P, Ca:P, Sr:P (Fig. 1; the component loadings are provided in the figure legend). These two sets of elements were considered separately because observations of the two sets of elements were frequently not paired and an aggregate consideration would precipitously decrease the sample size. The first two principal components account for 84.8% of the variance in transition metal data and 61.1% of the variance in the macronutrient and alkali and alkaline earth metal data.

The first principal component for the trace metals separates the observations by growth irradiance and accounts for 71% of the total variance in the data. Most metals are enriched relative to phosphorus, especially Fe, Mn, Cu, and Zn under low light, 15 and 30  $\mu\text{mol m}^{-2} \text{s}^{-1}$  quanta, and become increasingly depleted relative to phosphorus under irradiances saturating for growth, 250 and 500  $\mu\text{mol m}^{-2} \text{s}^{-1}$ . The species *T. weissflogii* and *P. provasolii* both have much lower metal enrichments at low light than the other species. The second principal component for the trace metals, dominated by Co:P, separates out subtle species-specific differences in metal composition. For the macronutrients and alkali and alkaline earth metals the first principal axis (~35% of the variance) also separates out different light treatments where many of the elements are relatively more enriched under low light, especially C:P, N:P, Mg:P, K:P, and Sr:P. The second principal component, especially C:P, N:P, and Ca:P, again highlights some of the differences between taxa.

The maximum variability in E:P (maximum minimum<sup>-1</sup> in E:P over all species and growth irradiances) is strongly correlated with its contribution to total cell mass (Fig. 2). C, N, and S all exhibit less than eightfold range in maximum minimum<sup>-1</sup> in E:P, the alkali and alkaline earth metals have about one order of magnitude range, and the trace metals tend to have a two to three order of magnitude range. A two-way ANOVA indicates that irradiance, taxonomic differences, and their interaction are all significant sources of variation in log (E:P),  $p < 0.001$  (Table 3). Phylogeny, irradiance, and the interaction between the two

in aggregate typically accounts for >80%, and often >90%, of the variation in the data. Among the macronutrients it is notable that a large proportion of the total variance in log (Mg:P), an element known to be affected by photoacclimation, is associated with the phenotypic response to irradiance. Similarly a large proportion of the total variance in many of the trace metals, especially log (Fe:P), log (Mn:P), log (Zn:P), log (Cu:P), and log (Mo:P), is associated with irradiance. In contrast, more of the variation in log (C:P), log (K:P), log (Ca:P), and log (Co:P) is explained by phylogenetic effects. The multiplicative interaction between phylogenetic effects and phenotypic response to irradiance was significant for all log (E:P) examined, tending to account for >30% of the total sum of squares.

*Functional response in E:P as a function of growth irradiance*—Most of the trace elements, Fe, Mn, Sr, Zn, Cu, Co, Mo, and the macronutrients, K and Mg, are enriched relative to phosphorus under irradiances that are limiting for growth. For some species, a select number of elements are also enriched relative to phosphorus at saturating irradiances, including Fe, Mn, and Zn in *T. weissflogii*, and Co in *Cyanothece* sp. and *P. provasolii*, suggestive of an increased species-specific requirement for these elements under saturating irradiance and high growth rates (Figs. 3, 4). In general, macronutrient:P did not change consistently with irradiance across the different species examined: C:P was high under saturating irradiance for *A. carterae* and high under low growth irradiance for *T. weissflogii* and *Cyanothece* sp.; N:P tended to decrease with irradiance for *T. weissflogii*, *Cyanothece* sp., and *A. carterae* but did not significantly change for *C. calcitrans* or *P. provasolii*. In contrast, log S:P and Ca:P have a maximum E:P at intermediate irradiance, ~100  $\mu\text{mol m}^{-2} \text{s}^{-1}$  quanta (Fig. 3).

*Functional response in the net rate of steady-state influx as a function of growth irradiance*—Previous studies have found that steady-state trace element uptake is a function of free metal availability in the media; therefore increases in

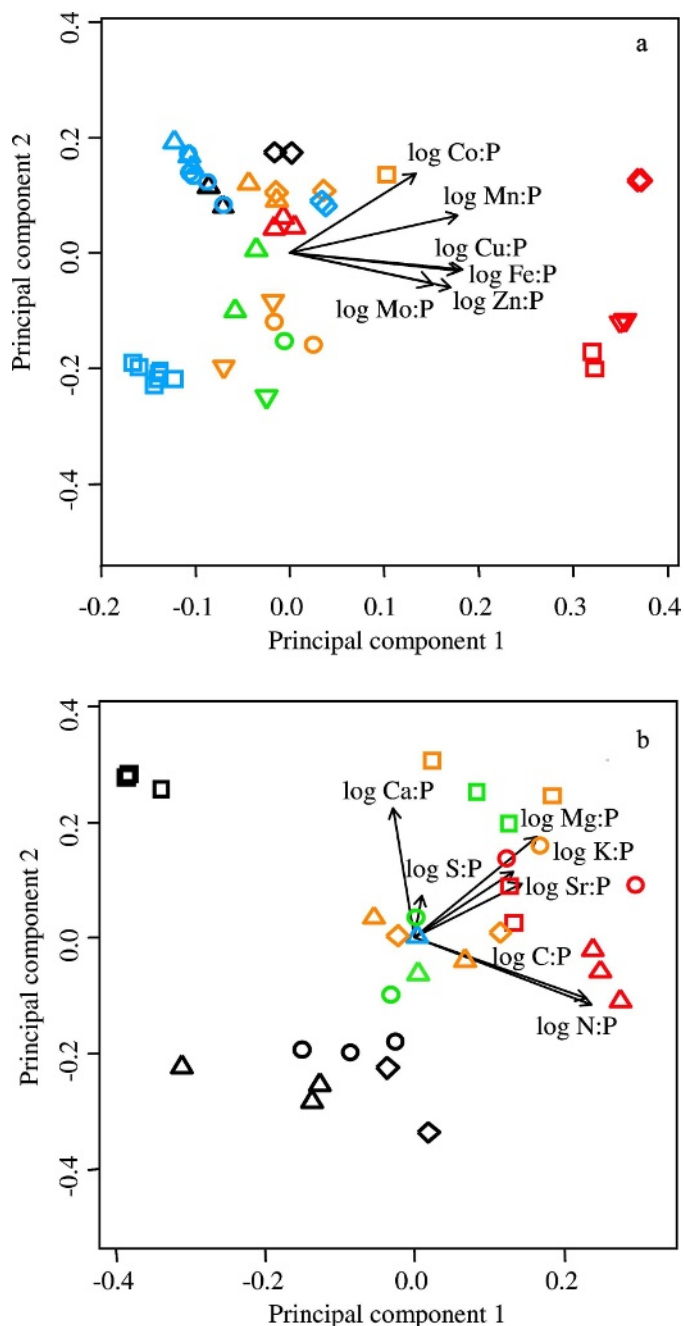


Fig. 1. Principal component analysis on correlations for: (A) the transition metals  $\log(\text{Fe}:\text{P})$ ,  $\log(\text{Mn}:\text{P})$ ,  $\log(\text{Zn}:\text{P})$ ,  $\log(\text{Cu}:\text{P})$ ,  $\log(\text{Co}:\text{P})$ ,  $\log(\text{Mo}:\text{P})$ . The first two components account for 84.8% of the data; principal component I is  $0.44 \log(\text{Fe}:\text{P}) + 0.44 \log(\text{Mn}:\text{P}) + 0.42 \log(\text{Zn}:\text{P}) + 0.45 \log(\text{Cu}:\text{P}) + 0.33 \log(\text{Co}:\text{P}) + 0.34 \log(\text{Mo}:\text{P})$  and principal component II is  $-0.20 \log(\text{Fe}:\text{P}) + 0.36 \log(\text{Mn}:\text{P}) - 0.35 \log(\text{Zn}:\text{P}) - 0.17 \log(\text{Cu}:\text{P}) + 0.77 \log(\text{Co}:\text{P}) - 0.30 \log(\text{Mo}:\text{P})$ ; (B) the macronutrients and alkali and alkaline earth metals,  $\log(\text{C}:\text{P})$ ,  $\log(\text{N}:\text{P})$ ,  $\log(\text{S}:\text{P})$ ,  $\log(\text{K}:\text{P})$ ,  $\log(\text{Mg}:\text{P})$ ,  $\log(\text{Ca}:\text{P})$ ,  $\log(\text{Sr}:\text{P})$ . The first two principal components account for 61.1% of the variance; principal component I is  $0.56 \log(\text{C}:\text{P}) + 0.57 \log(\text{N}:\text{P}) + 0.02 \log(\text{S}:\text{P}) + 0.31 \log(\text{K}:\text{P}) + 0.38 \log(\text{Mg}:\text{P}) - 0.08 \log(\text{Ca}:\text{P}) + 0.34 \log(\text{Sr}:\text{P})$  and principal component II is  $-0.29 \log(\text{C}:\text{P}) - 0.30 \log(\text{N}:\text{P}) + 0.21 \log(\text{S}:\text{P}) + 0.30 \log(\text{K}:\text{P}) + 0.49 \log(\text{Mg}:\text{P}) + 0.62 \log(\text{Ca}:\text{P}) + 0.27 \log(\text{Sr}:\text{P})$ . The color of the data points is used to represent light

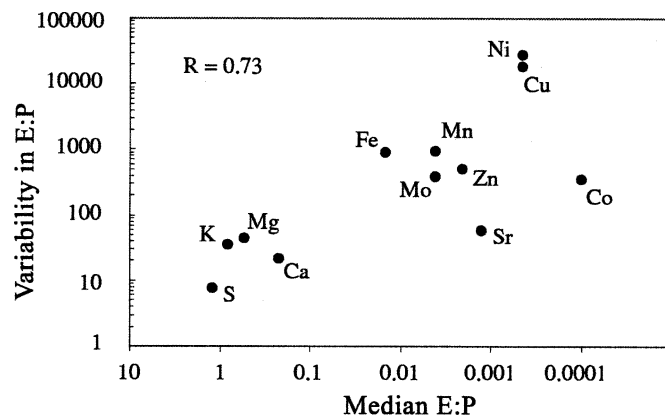
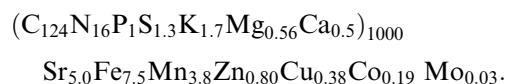


Fig. 2. Variability in  $(\text{maximum} \times \text{minimum}^{-1})$  in E:P as a function of total contribution to cellular biomass (median E:P). Macronutrients are reported as  $\text{mol mol}^{-1}$ , micronutrients  $\text{mmol mol}^{-1}$ .

growth rate with an increase in irradiance without a change in nutrient concentrations will result in a decrease in E:P or E:C, termed the growth dilution hypothesis (Sunda and Huntsman 1997). The steady-state net influx ( $\mu \times \text{E}:\text{P}$ ) for all the alkali and alkaline earth (except Ca) and transition elements is a function of irradiance (Table 4); this indicates that decreases in E:P are not only due to changes in growth rate, but active regulation in net steady-state nutrient influx as a function of growth and irradiance (Figs. 5, 6). As a result, Mn:P, Fe:P, Zn:P, Mo:P, and Co:P can increase about one order of magnitude and Cu:P more than three orders of magnitude under low versus high growth irradiance. For all species except *T. weissflogii*, the net steady-state rate of trace element influx for Fe, Mn, Cu, Co, Mo, and Mg is much higher under low irradiance ( $15$  and  $30 \mu\text{mol m}^{-2} \text{s}^{-1}$  quanta). In *T. weissflogii* the net steady-state rate of influx for Fe, Mn, Zn, Cu, and Co all increase relative to P at  $500 \mu\text{mol m}^{-2} \text{s}^{-1}$  relative to  $250 \mu\text{mol m}^{-2} \text{s}^{-1}$ . The net rate of steady-state influx of Ca and S tends to be elevated at intermediate irradiance, the maximum tending to occur  $\sim 100 \mu\text{mol m}^{-2} \text{s}^{-1}$ , but not for all species (Fig. 5).

## Discussion

Differences in elemental stoichiometry characterize different taxonomic groups grown under comparable environmental conditions (Ho et al. 2003; Quigg et al. 2003; Falkowski et al. 2004). Ho et al. (2003) defined an average elemental stoichiometry of nutrient-saturated marine phytoplankton grown at  $250 \mu\text{mol m}^{-2} \text{s}^{-1}$  as:



← treatments: 500 (black), 250 (blue), 100 (green), 30 (orange), and  $15 \mu\text{mol m}^{-2} \text{s}^{-1}$  quanta (red), and shapes represent species: triangle *T. weissflogii*, inverted triangle *C. calcitrans*, circles *P. provasolii*, diamonds *A. carterae*, and squares *Cyanothecae* sp.

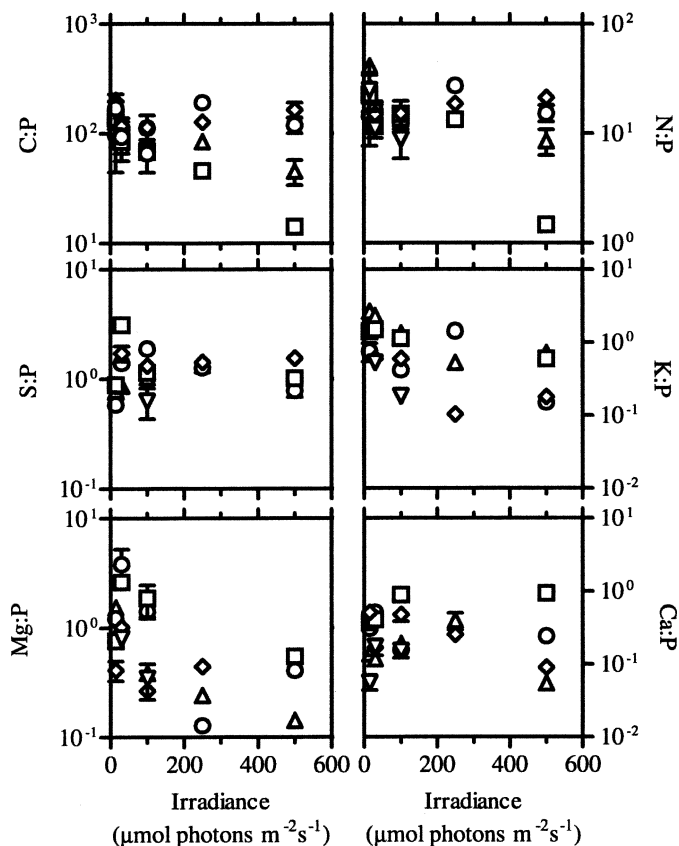
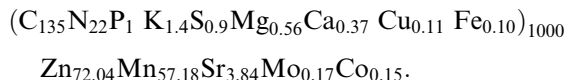


Fig. 3. Log (E:P) for the macronutrients and the alkali and alkaline earth metals ( $\pm 1$  SE) as a function of growth irradiance. The different species are denoted by symbols as in Fig. 1, units as in Table 1.

Note that Ni:P was not measured by Ho et al. (2003), but at  $250 \mu\text{mol m}^{-2} \text{s}^{-1}$  we found it ranged between species from 0.02 to 0.12 with an average of  $0.06 \text{ mmol mol}^{-1}$ . On the basis of the five species examined, over 15 to  $500 \mu\text{mol m}^{-2} \text{s}^{-1}$  quanta, phenotypic responses to irradiance is responsible for less than one to about three orders of magnitude in E:P within species, comparable to phylogenetic differences (Quigg et al. 2003), contrary to our original hypothesis, although phylogenetic effects are still clearly visible (Fig. 1). A change in irradiance alters the stoichiometry of several of these elements (Figs. 1, 3, 4; Table 1). In particular, many of the trace metals are highest at very low irradiance, Fe:P, Mn:P, Zn:P, Cu:P, Co:P, Mo:P, and Ni:P, whereas S:P, K:P, Mg:P, and Ca:P tend to be highest at intermediate irradiances. Irradiance thus has different effects on E:P in different species, often magnifying between-species differences in elemental stoichiometry. For example, the elemental stoichiometry of *Cyanothece* sp. at  $15 \mu\text{mol m}^{-2} \text{s}^{-1}$  is:



This example and the data in Table 1 indicate that the elemental stoichiometry of phytoplankton biomass may differ significantly between light-limited and light-saturated

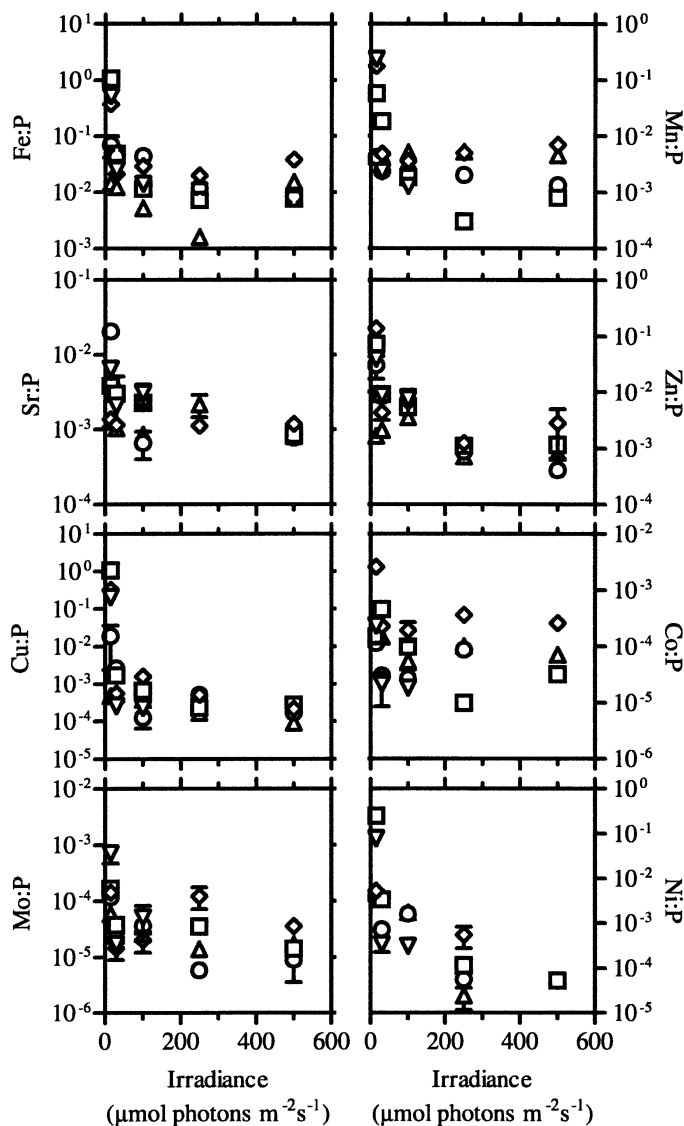


Fig. 4. Log (E:P) for the trace metals ( $\pm 1$  SE) as a function of growth irradiance. The different species symbols as in Fig. 1, units as in Table 1.

regions of the ocean because of both the phenotypic response to light and corresponding changes in the taxonomic composition of the communities.

*The role of photoacclimation in variation in E:P*—Phytoplankton regulate their metabolic rates in response to changes in incident irradiance through a variety of plastic physiological responses broadly referred to as photoacclimation. Although there are taxonomic differences in acclimation strategies, there are some general phenotypic physiological responses that are common to all species; for example cellular pigment concentration tends to increase with decreases in irradiance (Richardson et al. 1983; Falkowski and LaRoche 1991; MacIntyre et al. 2001). Many cellular components associated with photoacclimation have unique elemental stoichiometries that can alter the overall elemental stoichiometry of cells over a light

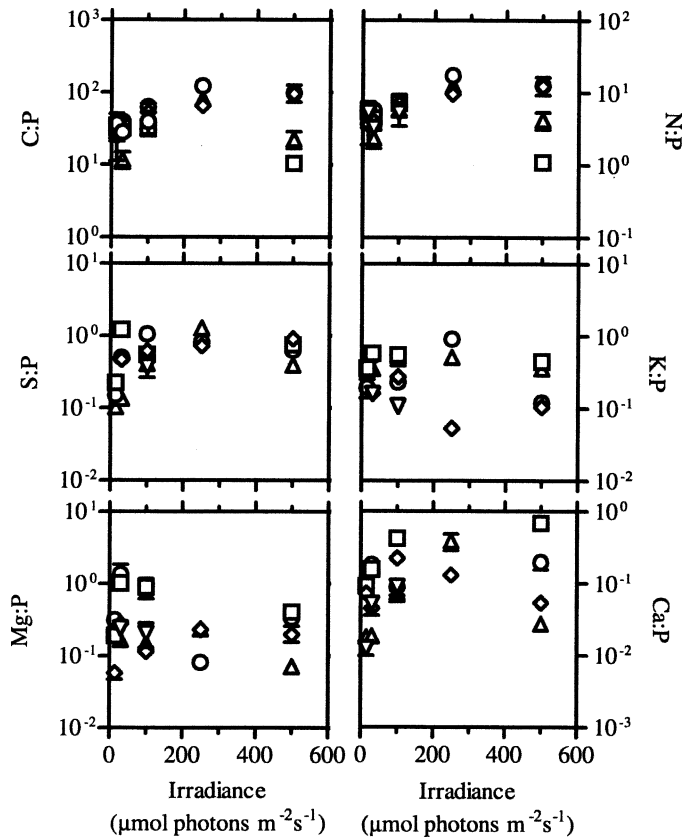


Fig. 5. Log steady-state net rate of influx for each macro-nutrient and the alkali and alkaline earth metal relative to P (log mol E  $\times$  [mol P  $\times$  h]<sup>-1</sup>) as a function of growth irradiance. Species symbols as in Fig. 1, units as in Table 1.

gradient (Raven 1988, 1990). For example, each chlorophyll *a* molecule has a Mg atom, so the change in pigment with irradiance results in a shift in Mg:P (Table 1), although, in contrast with trace elements, biophysical gradients across the cell membrane likely play a major role in controlling the intracellular concentrations of Mg, Ca, and K (on a fresh weight basis). On the basis of the decreasing efficiency of exciton transfer with the size of the light-harvesting antennae (at large antennae sizes), Raven (1988, 1990) estimated that photoacclimation to low irradiance can trigger an increased need for cellular Fe:P and Mn:P because of their requirement in the photosynthetic reaction centers, photosynthetic electron transport, and water splitting capacity, in agreement with field and laboratory measurements (Sunda and Huntsman 1997, 1998a). Increases in nitrogen (N:P) have also been observed and attributed to increased protein associated with increased cellular pigment (Sciandra et al. 1997; Flynn et al. 2001). In other studies, especially those where the experimental species were well acclimated to the growth irradiance, C:N:P did not change significantly with irradiance (Rhee and Gotham 1981; Goldman 1986; Leonardos and Geider 2004), in agreement with our observations. We found that a large number of elements, especially the trace metals, but not only those associated

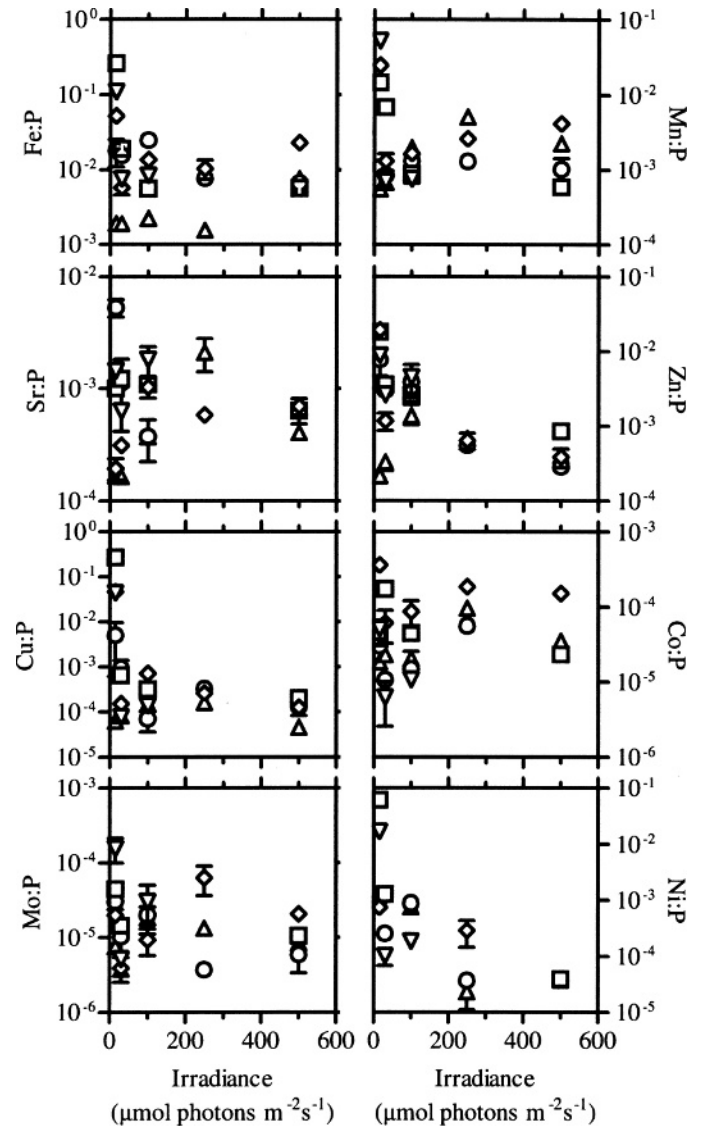


Fig. 6. Log steady-state net rate of influx for the trace metals relative to P (log mmol E  $\times$  [mol P  $\times$  h]<sup>-1</sup>) as a function of growth irradiance. Species symbols as in Fig. 1, units as in Table 1.

with light harvesting, became enriched relative to phosphorus under low growth irradiance. For a few species a select number of elements became enriched relative to phosphorus at saturating irradiances including Fe, Mn, and Zn in the coastal diatom *T. weissfloggi*, and Co in the diazotroph *Cyanothece* sp. and the prasinophyte, *P. provasolii*, perhaps indicating an increased requirement for these elements under saturating irradiance and high growth rates (Fig. 4). The large increases in Zn:P, Mo:P, Co:P, and Cu:P under low growth irradiance questions the interpretation that observed increases in total cellular Fe:P and Mn:P under low growth irradiance are due to metabolic requirements.

*Mechanistic models for E:P*—The growth rate hypothesis of Sterner and Elser (2002) predicts a decrease in N:P with increased growth rate because of an increased cellular



allocation of P to RNA synthesis to meet protein synthesis demand (Elser et al. 2000; Sterner and Elser 2002). There is accumulating evidence against the generality of the growth rate hypothesis, especially when phosphorus is not the limiting element (Elser et al. 2003; Ågren 2004). The growth rate hypothesis is based on the inference that an increase in growth requires an increase in the pool of cellular phosphorus; this differs from the theoretical calculations of Raven (1988, 1990), which explicitly consider the moles of element required to make a reaction run at a specific rate (but see Ågren 2004; Klausmeier et al. 2004). In this study the interspecific relationship between N:P and growth rate is weak (Table 1). Sunda and Huntsman (1997, 1998a,b, 2004) propose that

$$E : P = V/\mu \quad (1)$$

where  $V$  is the steady-state nutrient uptake or net influx of the element  $E$ . Sunda and Huntsman (1998) suggest that  $E:P$  is generally controlled by a feedback mechanism, and  $V$  increases with nutrient availability, resulting in increased cellular quota, which then leads to increased growth ( $\mu$ ) and eventually a decrease in  $E:P$ . There is an inherent assumption that the elements that compose a large proportion of cellular biomass, such as C and P, have cellular concentrations that are linearly related to growth rate. As a result this model predicts that under nutrient-saturating conditions an increase in growth rate due to irradiance will result in a decrease in cellular  $E:C$  or  $E:P$ . For *T. pseudonana* and *Prorocentrum minimum*, Sunda and Huntsman (1997, 1998a,b) found that  $Mn:C$  and  $Fe:C$  were independent of irradiance between 50 and 500  $\mu\text{mol m}^{-2} \text{s}^{-1}$  quanta, and that changes in  $E:C$  were primarily due to biodilution due to increased growth rate. Our observations contradict the result of Sunda and Huntsman under growth irradiances lower than those they tested.

*Re-evaluating the effect of irradiance on the mechanistic model for  $E:P$* —For five different species we find that below 50  $\mu\text{mol m}^{-2} \text{s}^{-1}$  quanta the steady-state net nutrient influx (Figs. 5, 6) for Fe, Mn, Zn, Cu, Co, Mo, Sr, and Mg are strongly affected by irradiance, resulting in a large accumulation of these  $E$  relative to P (and C) under low irradiance (Fig. 3). This accumulation does not occur proportionally over the range of irradiances; instead there is a radical increase in the above-mentioned  $E:P$  between the lowest irradiances, 15 and 30  $\mu\text{mol m}^{-2} \text{s}^{-1}$ , examined. This is not likely due to the effect of irradiance on the availability of free metal because an increase in irradiance would only increase the availability of Fe and the steady-state uptake, resulting in an underestimation of the steady-state uptake rate under low light (Sunda and Huntsman 1997, 1998a,b). This rapid accumulation of  $E:P$  under low irradiance has been previously reported for  $Fe:C$  in *T. weissflogii* and furthermore it was demonstrated that the observed accumulation of  $Fe:C$  under low light ( $<37 \mu\text{mol m}^{-2} \text{s}^{-1}$ ) was inconsistent with any reasonable accumulation of photosystems II and I, indicating that the large accumulation may be due to accumulation of the

trace element into a nonmetabolic pool (Strzepek and Price 2000).

Previously, increases in cellular  $Fe:P$  and  $Mn:P$  have been attributed to an increase in metabolic requirements for these elements under low light (Raven 1988, 1990; Sunda and Huntsman 2004). Although increased requirements for  $Fe:P$  and  $Mn:P$  are predicted on the basis of increased cellular concentrations of Fe and Mn-rich photosynthetic machinery, total cellular  $Fe:P$  and  $Mn:P$  do not necessarily reflect biochemical need. For most of the trace elements only a small proportion of their total cellular concentration has been identified in known metabolic processes (Hewitt 1983). Substantial cellular accumulation (for example, storage) could make it difficult to detect any patterns in elemental stoichiometry from whole cells. Storage vacuoles, such as the acidocalcisomes (polyphosphate vacuoles), are known to have associated quantities of a number of elements including Na, Mg, S, Cl, K, Ca, Zn, and Cd (Hall 2002; Docampo et al. 2005). On the basis of experimental data on storage of C, N, and P, Fogg and Thake (1987) hypothesized that the accumulation ability for a given nutrient will increase as its proportion of total cell mass decreases. For the species examined, the multiplicative range in  $E:P$  is correlated with log median  $E:P$  in biomass, suggesting an increased accumulation capacity for nutrients that make up a small proportion of cell biomass (Fig. 2). A large storage capacity for an element will make it extremely difficult to detect changes in its stoichiometry with other elements associated with metabolic requirements from measurements of whole cells. The large accumulation of trace metals relative to phosphorus under low growth irradiance is consistent with Strzepek and Price's (2000) hypothesis that there may be an increase in the storage of trace elements in nonmetabolic pools under very low growth irradiance. The storage of micronutrients may provide the cells and their progeny with a pool of micronutrients that can be exploited once the cells are exposed to saturating growth irradiance, or may be a competitive strategy used by phytoplankton to starve heterotrophs with overlapping nutrient requirements (Grover 2000).

The elemental stoichiometry of phytoplankton cells is the sum of  $E$  associated with metabolic requirements and cellular accumulation normalized by the sum of P or other normalizing element associated with metabolic requirements and cellular accumulation, or equivalently the relative rates of net steady-state influx (influx – efflux) of different nutrients into the cell:

$$\begin{aligned} \text{phytoplankton } E : P & \\ &= (\text{requirement}_E + \text{accumulation}_E) \\ &\quad \times (\text{requirement}_P + \text{accumulation}_P)^{-1} \quad (2) \\ &= (\text{influx}_E - \text{efflux}_E)(\text{influx}_P - \text{efflux}_P)^{-1}. \end{aligned}$$

To understand why the elemental stoichiometry of phytoplankton changes with irradiance, we need to evaluate how each of the quantities in Eq. 2 change with irradiance. There is very little information on how growth irradiance

affects the influx and efflux rates for different elements. Experimental studies of nutrient uptake suggest that an increase in growth irradiance increases the maximum rate of uptake,  $V_{\max}$  (Reshkin and Knauer 1979; Anderson and Roels 1981), which is often interpreted as an estimate of the maximum rate of net influx of a given nutrient. There is considerable species- and nutrient-specific variability in the irradiance dependence of  $V_{\max}$  (Eppley et al. 1971; Reshkin and Knauer 1979; Litchman et al. 2004), but experimental data support theoretical predictions that the light dependence of  $V_{\max}$  is most pronounced for nutrients that require relatively more energy to be assimilated (Litchman et al. 2004).

On the basis of the information available, the observed increase in E:P under low growth irradiance is as likely due to a decrease in efflux of E relative to P as to an increase in influx of E relative to P. On the basis of bacterial influx and efflux systems it has been hypothesized that it may be more energetically costly to restrict and select entry of different ions than induce efflux (Silver 1996). Observations of efflux in phytoplankton tend to be highly variable and related to factors that cause physiological stress including high irradiance (Zlotnik and Dubinsky 1989), supporting the hypothesis that efflux may be a quantitatively important process in determining the steady-state elemental stoichiometry of phytoplankton. Analyses of the relative costs and benefits of influx, efflux, and storage of different elements under different growth rates and growth irradiances would aid in interpreting the rather large accumulation of micronutrients relative to C, N, and P under low light. Alternatively, there is some evidence that some trace metal transporters are not very specific for a single metal, leading to complex antagonistic interactions. For example, Zn and Cu can be taken up incidentally by transporters for Fe and Mn (Bruland et al. 1991, and references therein), and may account for coordinated changes in many of the trace elements in response to irradiance.

The cycling and transport of Mn, Zn, Cd, Cu, and Fe can be greatly affected by phytoplankton in the upper water column (Sunda and Huntsman 1998a; Morel and Price 2003), but these effects are complicated by photochemical effects on redox cycling, hydrographic conditions, and the complex biological and chemical controls on the formation and destruction of organic complexes that bind to many of the trace metals (Knauer and Martin 1973; Morel and Price 2003). Knauer and Martin (1973) found increases in total dissolved Cd, Cu, Mn, and Zn associated with periods of upwelling that were, in some instances, followed by moderate decreases in Cd and Zn in the surface waters of Monterey Bay, California. Kudo and Matsunaga (1998) also found after the spring bloom in Funke Bay that although Cd and the macronutrients were removed from the euphotic zone, Ni and Cu exhibited very little change, suggesting that very large blooms may be required to measurably detect an effect on the total concentration of the soluble metals with a biological role in the phytoplankton (Knauer and Martin 1973; Kudo and Matsunaga 1998). Over the course of the spring bloom in South San Francisco Bay, California, large depletions observed in total dissolved Ni, Cd, and Zn, but not Cu, were associated

with decreases in the macronutrients Si and P (Luoma et al. 1998), indicating that environmental conditions associated with the bloom (such as high vertical mixing and exposure to low average irradiance) may account for high metal incorporation into phytoplankton biomass. Luoma et al. (1998) suggest that the differences in the inferred elemental stoichiometry of the phytoplankton from South San Francisco Bay versus open ocean plankton (Bruland et al. 1991) are likely due to differences in trace element availability in the different systems and the taxonomic composition of the plankton. Our results support the assertion that both differences in environmental conditions, irradiance, and nutrient concentration and stoichiometry (Bruland et al. 1991), and the taxonomic composition of the phytoplankton community can significantly affect the elemental stoichiometry of phytoplankton-derived particulate organic material and the corresponding depletion of dissolved nutrients.

The large phenotypic shift in the elemental composition of phytoplankton in response to growth irradiance indicates that phytoplankton may contribute to significant differences in the elemental composition of particulate matter between light-limited and light-saturated regions of the ocean. Significant proportions of phytoplankton biomass and export production may be light-limited and nutrient-saturated. It has been estimated that mesoscale eddies are responsible for 35–50% of new production,  $\sim 0.5 \text{ mol m}^{-2} \text{ yr}^{-1} \text{ N}$  (McGillicuddy et al. 1998). These eddies lift micro- and macronutrients into the lower portions of the euphotic zone, often stimulating the growth and export of light-limited phytoplankton, especially diatoms (Goldman and McGillicuddy 2003; Sweeney et al. 2003). Our observations of extremely high accumulation of Fe, Mn, Zn, Cu, Co, and Mo relative to P under very low irradiance suggest that areas characterized by eddies, intense vertical mixing, or a pronounced deep chlorophyll maxima should be examined for higher than typical Fe, Mn, Zn, Cu, Co, and Mo relative to P in particulate matter and corresponding depletion in the concentration of bioavailable dissolved concentrations of these elements.

The effects of low irradiance and taxonomic composition on elemental stoichiometry, especially Fe, Mn, Zn, Co, Cu, and Mo relative to P, are large and likely contribute to differences in the elemental stoichiometry of plankton and cycling in the ocean, but several factors may make it difficult to observe in a field setting. Changes in irradiance are often causally correlated with changes in macro- and micronutrient stoichiometry and concentration and changes in the taxonomic composition of the phytoplankton community, making it extremely difficult to identify any particular cause with a change in the elemental composition of particulate organic matter. In addition, the bioavailability of Fe, Co, Cd, Cu, and Zn is regulated in part by their reaction with organic complexing agents with mostly uncharacterized low molecular mass ligands that are likely associated with metal sequestration, detoxification, and in some cases transport into phytoplankton cells, and photochemically affected redox cycling contributes to the biological availability and distribution of Fe, Mn, Cu, and

Co (Sunda and Huntsman 1998a; Morel and Price 2003). For example, depletion of  $\text{Cu}^{2+}$  and  $\text{Mn}^{2+}$  reported in deep chlorophyll maxima (Moffett 1995; Sunda and Huntsman 1998a) is consistent with our observations, but has been attributed primarily to these other factors. Using adsorptive cathodic stripping voltammetry, Moffett (1995) found very low free cupric ion concentration in samples collected from the Bermuda Atlantic Time Series Station following periods of intense vertical mixing and associated with the deep chlorophyll maximum in the Sargasso Sea. The bioavailability of cupric ion is controlled by ligand (L1) concentrations that likely act to prevent Cu toxicity, especially for sensitive phytoplankton species. Cu accumulation in phytoplankton under low light is consistent with the variable relationship between cell density of *Synechococcus* and *Prochlorococcus* and ligand (L1) concentrations (Moffett 1995), especially after intense vertical mixing and in the deep chlorophyll maximum.  $\text{Mn}^{2+}$  tends to decrease with depth in the surface; this profile has been attributed to a combination of photodissociation associated with Mn redox cycling and atmospheric inputs (Sunda and Huntsman 1998a and references therein), although low-light-enhanced accumulation in phytoplankton biomass may also contribute to this characteristic vertical distribution. Ideally, evidence for low-light trace element enrichment relative to P in phytoplankton biomass should come from simultaneous measurements of the free dissolved elemental composition of the water column, the elemental stoichiometry of the particulate matter in different size fractions and size-fractionated high-performance liquid chromatography determination of total chlorophyll, and taxonomic composition complemented by microscopic identification of taxa with depth in stratified and well-mixed water columns. If high phytoplankton biomass is responsible for, even in part, the observed depletion of trace elements such as  $\text{Cu}^{2+}$  and  $\text{Mn}^{2+}$  in deep chlorophyll maxima, we would expect similar patterns of depletion in other trace metal profiles, most likely bioavailable Fe, Zn, and Co. Since the trends in trace element enrichment under low light are to some degree taxon specific, we hypothesize that there may be differences in the stoichiometry of trace element depletion in regimes where the deep chlorophyll maximum is composed of different algal groups. Overall these results suggest that the fractionation of trace metals relative to phosphorus and carbon in light-limited, nutrient-saturated phytoplankton may be a very important and previously unrecognized component of the biogeochemical cycling of trace elements in the ocean.

## References

- ÅGREN, G. I. 2004. The C:N:P stoichiometry of autotrophs—theory and observations. *Ecol. Lett.* **7**: 185–191.
- ANDERSON, S. M., AND O. A. ROELS. 1981. Effects of light intensity on nitrate and nitrate uptake and excretion by *Chaetoceros curvisetus*. *Mar. Biol.* **62**: 257–261.
- BRULAND, K. W., J. R. DONAT, AND D. A. HUTCHINS. 1991. Interactive influences of bioactive trace metals on biological production in oceanic waters. *Limnol. Oceanogr.* **38**: 1555–1577.
- BRZEZINSKI, M. A. 1985. The Si:C:N ratio of marine diatoms: Interspecific variability and the effect of some environmental variables. *J. Phycol.* **21**: 347–357.
- DOCAMPO, R., W. DESOUSA, K. MIRANDA, P. ROHLOFF, AND S. N. J. MORENO. 2005. Acidocalcisomes—conserved from bacteria to man. *Nature Rev. Microbiol.* **3**: 251–261.
- , AND OTHERS. 2000. Biological stoichiometry from genes to ecosystems. *Ecol. Lett.* **3**: 540–550.
- ELSER, J. J., AND OTHERS. 2003. Growth rate–stoichiometry couplings in diverse biota. *Ecol. Lett.* **6**: 936–943.
- EPPLEY, R. W., J. N. ROGERS, J. J. MCCARTHY, AND A. SOURNIA. 1971. Light/dark periodicity in nitrogen assimilation of the marine phytoplankters *Skeletonema costatum* and *Coccolithus huxleyi* in N-limited chemostat culture. *J. Phycol.* **7**: 150–154.
- FALKOWSKI, P. G. 2000. Rationalizing elemental ratios in unicellular algae. *J. Phycol.* **36**: 3–6.
- , M. E. KATZ, A. H. KNOLL, A. S. QUIGG, J. A. RAVEN, O. SCHOFIELD, AND F. J. R. TAYLOR. 2004. The evolution of modern eukaryotic phytoplankton. *Science* **305**: 354–360.
- , AND J. LAROCHE. 1991. Acclimation to spectral irradiance in algae. *J. Phycol.* **27**: 8–14.
- FLEMING, R. H. 1940. Composition of plankton and units for reporting populations and production, p. 535–539. Proceedings of the sixth Pacific science congress of the Pacific science association. 1939. University of California Press.
- FLYNN, K. J., H. MARSHALL, AND R. J. GEIDER. 2001. A comparison of two N-irradiance interaction models of phytoplankton growth. *Limnol. Oceanogr.* **46**: 1794–1802.
- FOGG, G. E., AND B. THAKE. 1987. Algal cultures and phytoplankton ecology. University of Wisconsin Press.
- GOLDMAN, J. C. 1986. On phytoplankton growth rates and particulate C:N:P ratios at low light. *Limnol. Oceanogr.* **31**: 1358–1363.
- , AND D. J. MCGILICUDDY, JR. 2003. Effect of large marine diatoms growing at low light on episodic new production. *Limnol. Oceanogr.* **48**: 1176–1182.
- GROVER, J. P. 2000. Resource competition and community structure in aquatic micro-organisms: Experimental studies of algae and bacteria along a gradient of organic carbon to inorganic phosphorus supply. *J. Plankton Res.* **22**: 1591–1610.
- HALL, J. L. 2002. Cellular mechanisms for heavy metal detoxification and tolerance. *J. Exp. Bot.* **53**: 1–11.
- HEWITT, E. J. 1983. A perspective of mineral nutrition: Essential and functional minerals in plants, p. 277–323. In D. A. Robb and W. S. Pierpoint [eds.], *Metals and micronutrients, uptake and utilization by plants*. Academic Press.
- HO, T.-Y., A. QUIGG, Z. V. FINKEL, A. J. MILLIGAN, K. WYMAN, P. G. FALKOWSKI, AND F. M. M. MOREL. 2003. Elemental composition of some marine phytoplankton. *J. Phycol.* **39**: 1145–1159.
- KLAUSMEIER, C. A., E. LITCHMAN, T. DAUFRESNE, AND S. A. LEVIN. 2004. Optimal nitrogen-to-phosphorus stoichiometry of phytoplankton. *Nature* **429**: 171–174.
- KNAUER, G. A., AND J. H. MARTIN. 1973. Seasonal variations of cadmium, copper, manganese, lead and zinc in water and phytoplankton in Monterey Bay, California. *Limnol. Oceanogr.* **18**: 597–604.
- KUDO, I., AND K. MATSUNAGA. 1998. Behavior of Cu, Ni and Cd during nutrient depletion in a spring bloom in Funka Bay. *J. Oceanogr.* **54**: 619–627.
- LEONARDOS, N., AND R. J. GEIDER. 2004. Effects of nitrate:phosphate supply ratio and irradiance on the C:N:P stoichiometry of *Chaetoceros muelleri*. *Eur. J. Phycol.* **39**: 173–180.

- LITCHMAN, E., C. A. KLAUSMEIER, AND P. BOSSARD. 2004. Phytoplankton nutrient competition under dynamic light regimes. *Limnol. Oceanogr.* **49**: 1457–1462.
- LUOMA, S. N., A. VAN GEEN, B.-G. LEE, AND J. E. CLOERN. 1998. Metal uptake by phytoplankton during a bloom in South San Francisco Bay: Implications for metal cycling in estuaries. *Limnol. Oceanogr.* **43**: 1007–1016.
- MACINTYRE, H. L., T. M. KANA, T. ANNING, AND R. J. GEIDER. 2001. Photosynthesis irradiance response curves and photosynthetic pigments in microalgae and cyanobacteria. *J. Phycol.* **38**: 17–38.
- MARTIN, J. H. 1992. Iron as a limiting factor in oceanic productivity, p. 123–137. *In* P. Falkowski and A. Woodhead [eds.], *Primary productivity and biogeochemical cycles in the sea*. Plenum.
- MCGILLICUDDY, D. J., AND OTHERS. 1998. Influence of mesoscale eddies on new production in the Sargasso Sea. *Nature* **394**: 263–266.
- MOFFETT, J. W. 1995. Temporal and spatial variability of copper complexation by strong chelators in the Sargasso Sea. *Deep-Sea Res. I* **42**: 1273–1295.
- MOREL, F. M. M., AND N. M. PRICE. 2003. The biogeochemical cycles of trace metals in the oceans. *Science* **300**: 944–947.
- QUIGG, A., AND OTHERS. 2003. The evolutionary inheritance of elemental stoichiometry in marine phytoplankton. *Nature* **425**: 291–294.
- R DEVELOPMENT CORE TEAM. 2005. R: A language and environment for statistical computing. R Foundation for Statistical Computing.
- RAVEN, J. A. 1988. The iron and molybdenum use efficiencies of plant growth with different energy, carbon and nitrogen sources. *New Phytol.* **109**: 279–287.
- . 1990. Predictions of Mn and Fe use efficiencies of phototrophic growth as a function of light availability for growth and of C assimilation pathway. *New Phytol.* **116**: 1–18.
- REDFIELD, A. C. 1934. On the proportions of organic derivatives in sea water and their relation to the composition of plankton, p. 176–192. *In* R. J. Daniel [ed.], *James Johnstone Memorial Volume*. Liverpool Univ. Press.
- . 1958. The biological control of the chemical factors in the environment. *Am. Sci.* **46**: 205–221.
- REINFELDER, J. R., AND N. S. FISHER. 1991. The assimilation of elements ingested by marine copepods. *Science* **251**: 794–796.
- RESHKIN, S. J., AND G. A. KNAUER. 1979. Light stimulation of phosphate uptake in natural assemblages of phytoplankton. *Limnol. Oceanogr.* **24**: 1121–1124.
- RHEE, G.-Y., AND I. J. GOTHAM. 1981. The effect of environmental factors on phytoplankton growth: Light and the interactions of light with nitrate limitation. *Limnol. Oceanogr.* **26**: 649–659.
- RICHARDSON, K., J. BEARDALL, AND J. A. RAVEN. 1983. Adaptation of unicellular algae to irradiance: An analysis of strategies. *New Phytol.* **93**: 157–191.
- SANUDO-WILHELMY, S. A., A. TIVAR-SANCHEZ, F.-X. FU, D. G. CAPONE, E. J. CARPENTER, AND D. A. HUTCHINS. 2004. The impact of surface-adsorbed phosphorus on phytoplankton Redfield stoichiometry. *Nature* **432**: 897–901.
- SCIANDRA, A., AND OTHERS. 1997. Growth-compensating phenomena in continuous cultures of *Dunaliella tertiolecta* limited simultaneously by light and nitrate. *Limnol. Oceanogr.* **42**: 1325–1339.
- SILVER, S. 1996. Bacterial resistances to toxic metal ions—a review. *Gene* **179**: 9–19.
- SOKAL, R. R., AND F. J. ROHLF. 1994. *Biometry: The principles and practice of statistics in biological research*, 3rd ed. W. H. Freeman.
- STERNER, R. W., AND J. J. ELSER. 2002. *Ecological stoichiometry: The biology of the elements from molecules to the biosphere*. Princeton University Press.
- STRZEPEK, R. F., AND N. M. PRICE. 2000. Influence of irradiance and temperature on the iron content of the marine diatom *Thalassiosira weissflogii* (Bacillariophyceae). *Mar. Ecol. Prog. Ser.* **206**: 107–117.
- SUNDA, W. G., AND S. A. HUNTSMAN. 1997. Interrelated influence of iron, light and cell size on marine phytoplankton growth. *Nature* **390**: 389–392.
- , AND ———. 1998a. Interactive effects of external manganese, the toxic metals copper and zinc, and light in controlling cellular manganese and growth in a coastal diatom. *Limnol. Oceanogr.* **43**: 1467–1475.
- , AND ———. 1998b. Processes regulating cellular metal accumulation and physiological effects: Phytoplankton as model systems. *Sci. Total Environ.* **219**: 165–181.
- , AND ———. 2004. Relationships among photoperiod, carbon fixation, growth, chlorophyll *a*, and cellular iron and zinc in a coastal diatom. *Limnol. Oceanogr.* **49**: 1742–1753.
- SWEENEY, E. N., D. J. MCGILLICUDDY, AND K. O. BUESSELER. 2003. Biogeochemical impacts due to mesoscale eddy activity in the Sargasso Sea as measured at the Bermuda Atlantic Time Series (BATS) site. *Deep-Sea Res. II* **50**: 3017–3039.
- ZLOTNIK, I., AND Z. DUBINSKY. 1989. The effect of light and temperature on DOC excretion by phytoplankton. *Limnol. Oceanogr.* **34**: 831–839.

Received: 3 June 2005

Accepted: 17 July 2006

Amended: 27 June 2006